Magnetic properties of square Py nanowires: Irradiation dose and geometry dependence

A. Ehrmann, T. Blachowicz, S. Komraus, M.-K. Nees, P.-J. Jakobs, H. Leiste, M. Mathes, and M. Schaarschmidt

Articles you may be interested in

Anisotropic magnetic properties of bi-layered structure of ordered Co nanowire array: Micromagnetic simulations and experiments
J. Appl. Phys. 114, 173905 (2013); 10.1063/1.4829034

Magnetic-field-orientation dependent magnetization reversal and spin waves in elongated permalloy nanorings
J. Appl. Phys. 108, 053909 (2010); 10.1063/1.3475648

Surface magnetization processes in soft magnetic nanowires
J. Appl. Phys. 107, 09E315 (2010); 10.1063/1.3360209

Magnetization reversal in nanowires with a spiral shape
J. Appl. Phys. 104, 013906 (2008); 10.1063/1.2948939

Systematic tuning of magnetization reversal in Permalloy nanowires using sloped ends
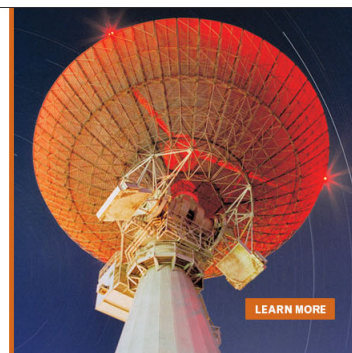J. Appl. Phys. 101, 09F510 (2007); 10.1063/1.2710958

Magnetic properties of square Py nanowires: Irradiation dose and geometry dependence

A. Ehrmann,[1,a)] T. Blachowicz,[2] S. Komraus,[2] M.-K. Nees,[3] P.-J. Jakobs,[3] H. Leiste,[3] M. Mathes,[4] and M. Schaarschmidt[4]

[1]*Faculty of Engineering Sciences and Mathematics, Bielefeld University of Applied Sciences, 33609 Bielefeld, Germany*
[2]*Institute of Physics – Center for Science and Education, Silesian University of Technology, 44-100 Gliwice, Poland*
[3]*Karlsruhe Nano Micro Facility (KNMF), Karlsruhe Institute of Technology (KIT), 76344 Eggenstein-Leopoldshafen, Germany*
[4]*ACCESS e. V., 57072 Aachen, Germany*

Arrays of ferromagnetic patterned nanostructures with single particle lateral dimensions between 160 nm and 400 nm were created by electron-beam lithography. The fourfold particles with rectangular-shaped walls around a square open area were produced from permalloy. Their magnetic properties were measured using the longitudinal magneto-optical Kerr effect. The article reports about the angle-dependent coercive fields and the influence of the e-beam radiation dose on sample shapes. It is shown that a broad range of radiation dose intensities enables reliable creation of nanostructures with parameters relevant for the desired magnetization reversal scenario. The experimental results are finally compared with micromagnetic simulations to explain the findings. © 2015 AIP Publishing LLC. [http://dx.doi.org/10.1063/1.4919839]

I. INTRODUCTION

Nanostructured magnetic particles belong to the important topics of recent research due to their possible application in magneto-electronic devices. In low-dimensional magnetic structures, the shape anisotropy significantly competes with magneto-crystalline and magneto-elastic anisotropies. Such structures allow for tailoring anisotropies and other magnetic properties by proper design of magnetic particles.[1] It also enables creation of exotic magnetic states. These effects were tested in research laboratories over the last few years. For example, round disks or dots show vortex states[2–4] which were used to define magnetic states due to the vortex core direction. Flux-closed vortex states, occurring in rings with the core region excluded, had strongly reduced stray fields, which evokes interest for data storage devices.[5,6] In large rectangular permalloy (Py) rings of $1 \mu m \times 1.5 \mu m$ (Ref. 7) or $0.7 \mu m \times 1.15 \mu m$,[8] respectively, stable onion states were found; in the case of a ring array structure, the transition between onion and vortex states is influenced by the packing density of the rings. Similar collective effects were observed in closely packed square Py lattices and six fold iron lattices,[9,10] where horseshoe and vortex states were attributed to sublattices with parallel or anti-parallel magnetic order. More magnetic states were reported for deformed cobalt ellipses of $660 nm \times 880 nm$,[11] and for permalloy square rings,[12] where onion, horseshoe, vortex, and domain wall states were observed. Among other shapes rectangles and triangles,[13] wires,[14] and tubes[15] as well as less geometric 2D forms were examined. 3D forms, such as cylinders[16] or thin bowls grown with diameters of 20 nm to 1000 nm on self-organizing non-magnetic half-spheres, also showed new interesting behavior with mixed in-plane and out-of-plane magnetization components, the latter being more pronounced for smaller half spheres.[17–19]

In a recent theoretical work by the authors,[20] it was shown that square nanowire systems can lead to stable intermediate states at remanence, which have been also reported for exchange bias systems,[21] enabling the use of such systems as quaternary memory cell (i.e., 2 bits per storage position). Further simulations have shown that the magnetic properties and magnetization dynamics of such nanostructured systems strongly depend on the lateral dimensions of the system as well as on the wire diameters.[22]

This article aims at investigating the influence of the lateral dimensions, tailored by e-beam lithography, of a real fourfold magnetic structures made with lateral dimensions between 160 nm and 400 nm. The shape of the samples presented can be classified between magnetic rings with their vortices and fourfold wire systems with the possibility of a stable intermediate state for a zero-valued externally applied magnetic field. Such a state is of large interest for possible applications in magnetic memories since it enables the creation of two-bit-per-storage-place media, using four instead of two stable states, resulting in doubling the possible data density in bit-patterned media.[20] Importantly, the influence of the wall diameter was tested by structuring samples with different electron-beam radiation doses, resulting in a variety of wall widths. In Secs. II and III, we present the lithographically obtained sample shapes as well as hysteresis loops measured by the longitudinal Magneto-Optical Kerr Effect (MOKE). Discussion of experimental results is supported by micromagnetic simulations. Finally, conclusions are provided.

---

a)Author to whom correspondence should be addressed. Electronic mail: andrea.ehrmann@fh-bielefeld.de

117, 173903-1

II. TECHNOLOGY AND MATERIALS

The samples are prepared by a lift-off process in the Karlsruhe Nano Micro Facility (KNMF). For this, a 4 in. silicon (100) wafer was spin-coated with a double layer resist of PMMA600k and PMMA950k on top. The pattern was exposed by the E-beam tool VB6UHR-EWF (Raith) with 100 keV energy. In order to tailor sample dimensions, the exposure dose was adjusted in steps of $40 \, \mu C/cm^2$, starting from $500 \, \mu C/cm^2$ up to $700 \, \mu C/cm^2$, using also the Proximity Effect Correction (PEC) procedure. A spraying tool with a solution of MIBK:IPA (1:3) was used as a developing tool. Finally, the substrates were metalized with 5 nm titan 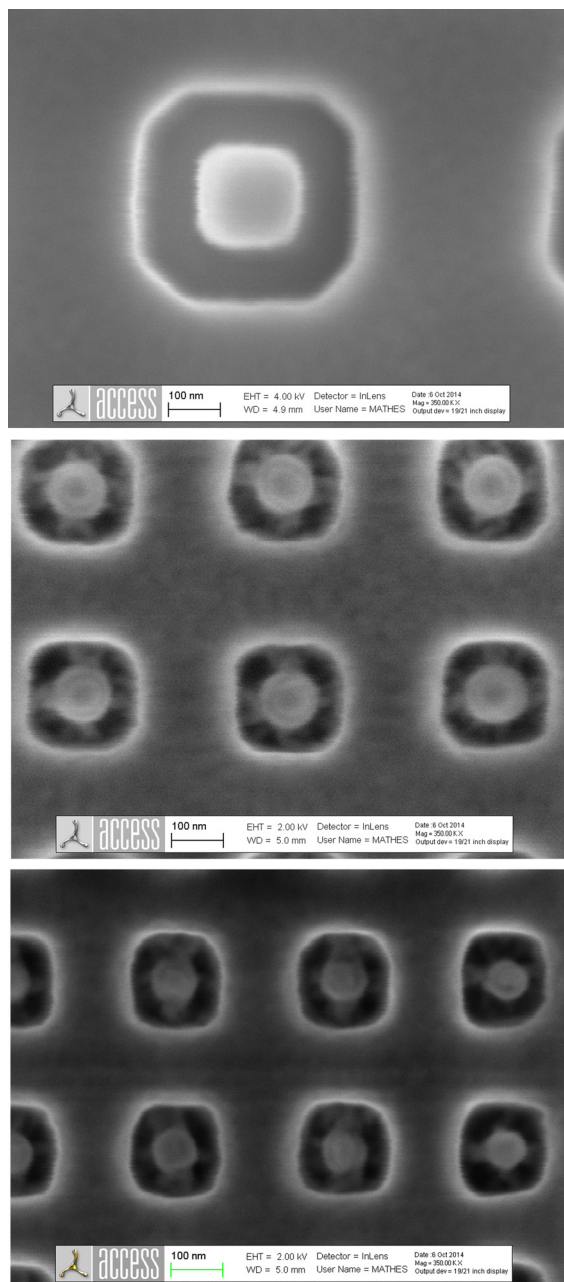layer as an adhesion promoter, followed by a 15 nm permalloy layer and a 1–2 nm titan cap layer. In the last step, the resist was stripped.

The sample shape was defined as a set of squares with sizes between 160 nm and 400 nm (Fig. 1). The distances between the single magnetic particles were identical to their sizes, and they were oriented in square matrixes of dimension $400 \, \mu m \times 400 \, \mu m$. The width of the wall width was tailored by the applied radiation dose, with the nominal value equal to $1/4$ of the wall length (Fig. 2).

In order to identify the resultant magnetic behavior, the in-plane angle-dependent coercive-fields were measured by the longitudinal MOKE. The samples were rotated with respect to the external magnetic field with an angular accuracy of $\pm 0.5°$. Signals were detected using the photodiode-bridge technique,[21] allowing for exact measurements of longitudinal magnetization components. The magnetic field was swept between ± 55 mT to reach saturated magnetization states.

Fig. 3 shows the results for samples of 400 nm size influenced by radiation doses of $500 \, \mu C/cm^2$–$700 \, \mu C/cm^2$. For these sample, three "regimes" can be recognized: the middle range ($580 \, \mu C/cm^2$–$660 \, \mu C/cm^2$) leading to characteristic angular-dependencies of the coercivity with maximum around $45°$; next, the lower range of radiation doses ($\leq 540 \, \mu C/cm^2$), causing a broadening of the angular dependency, and finally leading to splitting of coercivity maximum for the $500 \, \mu C/cm^2$ dose. At last, for the high radiation dose regime ($700 \, \mu C/cm^2$), the angular region between $35°$ and $55°$ shows a completely different magnetization reversal process, depicted by the rapid jumps in the angular-dependent curve at $30°$. This change in the magnetic behavior can be attributed to a specific magnetization reversal mechanism in the samples with the modified shape.

Fig. 4 provides a comparison of samples with three different sizes (160 nm, 200 nm, and 400 nm), each structured with a middle radiation dose of $580 \, \mu C/cm^2$. The coercivities become smaller for larger samples, which correspond to the fact that the shape anisotropy, blocking magnetization reversal processes in smaller particles,[23] has less influence in the larger
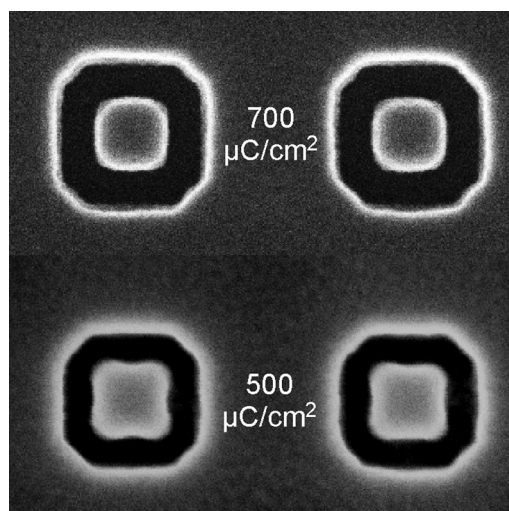

FIG. 1. SEM pictures of samples nanostructured with a radiation dose of $580 \, \mu C/cm^2$, with diameters 400 nm (top panel), 200 nm (middle panel), and 160 nm (bottom panel).

FIG. 2. The influence of radiation doses on 400 nm samples resulting in a reduction of the wall widths for the lowest dose of $500 \, \mu C/cm^2$.
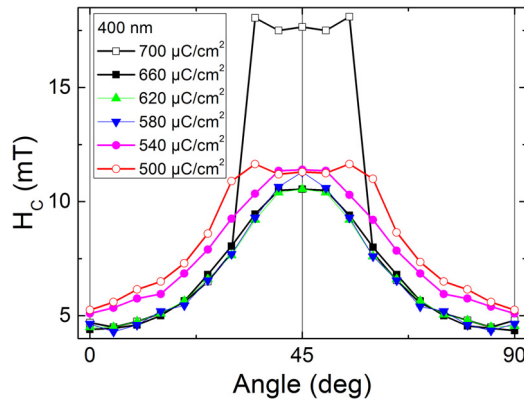
FIG. 3. Coercive fields measured by MOKE for the 400 nm samples treated with different e-beam radiation doses.
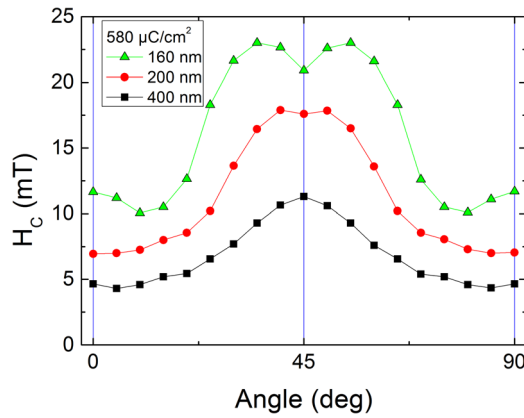

FIG. 4. Comparison of angle-dependent coercive fields H_C for arrays of samples with three different dimensions, structured with a radiation dose of 580 μC/cm^2. Samples of greater dimensions have better defined connections between walls at the corners.

samples, allowing for easier magnetization reversal. A splitting of the maximum around 45° for smaller samples is again visible.

III. DISCUSSION OF RESULTS

In order to understand experimental results, the SEM pictures were adopted in tetrahedral finite elements (FE) mesh models, to simulate narrower and wider walls of samples. The models were simulated by the Parallel Finite Element Micromagnetics Package (MAGPAR),[24] a micromagnetic solver based on the Landau-Lifshitz-Gilbert equation of motion using a Krylov subspace method, utilizing Adams-Moulton or BDF (backward differentiation formula) for non-stiff or stiff problems, respectively. In simulations, we employed the exchange constant A equal to 1.3×10^{-11} J/m, the magnetic polarization at saturation J_s equal to 1 T, and the phenomenological Gilbert damping constant α equal to 0.01. The used mesh size of 3 nm was comparable with the exchange length of permalloy (Figs. 5(a) and 5(b)) and the maximum spin angle is below 0.5 rad.

Fig. 5(c) shows the respective results. For the sample with the non-regular walls, equivalent to the 400 nm (500 μC/cm^2) case, the angle dependence of the simulated coercivity fits nearly perfectly with the measured behavior depicted in Fig. 3. For the sample with more regular walls, the simulation is nearly identical to the middle-regime range measurements.

A detailed look into the simulated hysteresis curve can help to understand the experimental angular-dependent behavior of hysteresis loops. In the simulation of the non-regular system, magnetization reversal at a sample orientation at 45° occurs by a flux-closed vortex state which is reached through chaotic, asymmetric domain wall processes. These are combinations of typical magnetization vortex-based reversal processes taking place in nano-rings and domain wall evolutions typical for nano-wires. In other words,
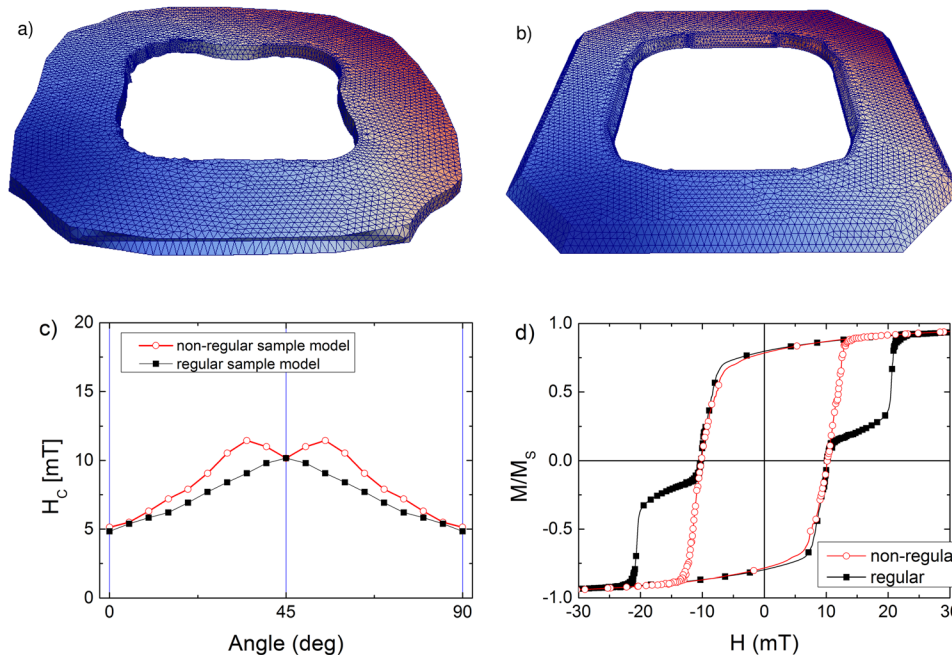

FIG. 5. Coercive fields, simulated for virtual samples of 400 nm size, in the non-regular (a) and regular (b) wall-shape regimes following the real samples created by the lowest and highest radiation doses, respectively (c). Hysteresis loops simulated for 45° orientation of virtual samples (d).
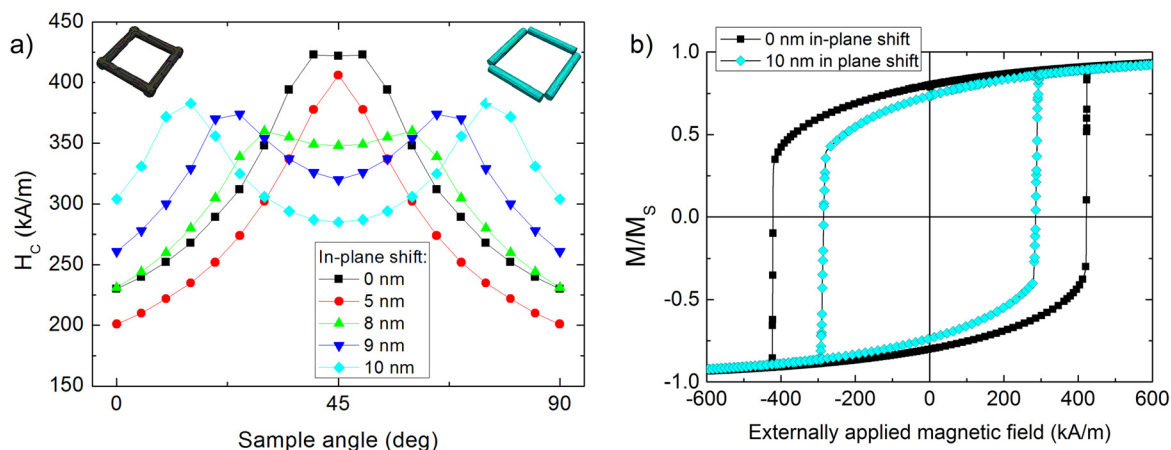
FIG. 6. Micromagnetic simulation of angle-dependent coercivities of wire systems with different corner connections between the wires (a); respective hysteresis loops simulated for a 45° sample orientation with 0 nm and 10 nm in-plane shifts (b).

this combined state can be interpreted as a deformed vortex. For a comprehensive review of these states see Refs. 20 and 22, while a comparative analysis between deformed and non-deformed samples is performed in Ref. 25.

In the more regular wall system, magnetization reversal happens principally in the same way; however, the vortex is significantly more stable and uniform for a relatively broad range of field intensities—while the vortex occurs only in a relatively smaller field range for the non-regular wall sample. This difference is seen as extended curve with steps on both sides of the hysteresis loop, related to the more stable vortices (Fig. 5(d)). In realistic systems, this leads to a reduced coercivity (see 540–600 $\mu C/cm^2$ cases in Fig. 3); however, for very strong radiation doses, it can lead to a significantly enhanced coercivity (comp. the 700 $\mu C/cm^2$ case in Fig. 3), depending on the exact magnetization value where the "step" starts (i.e., the "height" of the step), since experiments will detect either the "inner" or the "outer" slope of the hysteresis loop as coercive field. Importantly, from an applied point of view, this finding shows that a proper use of radiation doses leads to samples with desired magnetization reversal scenario.

An additional interesting factor, worth to be considered from a sample shape-regularity perspective, is the quality of wall connections at corners. To test this issue, we have performed micromagnetic simulations of similar wire systems with the wires being connected differently at the corners (Fig. 6). While for a complete crossover of the wires (black squares, upper left inset), only one extended maximum around 45° is visible in the simulation, decreasing the connections by more than 5 nm leads to a splitting of this maximum. This change of the connection character confirms the role of the wire-based processes which can decouple for reduced corners uniformity. Moreover, in the nearly unconnected sample (the 10 nm case in Figs. 6(a) and 6(b)) domain walls nucleate and propagate independently in the four wires, while in the sample with completely immersing wires (the 0 nm case in Figs. 6(a) and 6(b)), the magnetization reversal processes evolve through all-encompassing domain patterns seen as a single maximum in the angular-dependent coercivity. Similarly, thinner nanostructured system, obtained for

smaller e-beam doses, with accordingly decreased crossing at corners, reveal a characteristic splitting of the coercivity field maximum around 45°.

IV. CONCLUSIONS

In summary, we have shown experimentally the quantitative and qualitative changes in the angular-dependence of the coercive fields of square nanostructures with different lateral dimensions modified by e-beam lithography doses. Associated effects resulting from the wall widths and quality of corner regions can influence the magnetization reversal processes, hysteretic behavior, and coercive fields. This result enables tailoring the desired magnetic properties of patterned nanostructures by lithography with high reliability.

[1] J. Nogués, J. Sort, V. Langlais, V. Skumryev, S. Surinach, J. S. Munoz, and M. D. Baro, Phys. Rep. **422**, 65 (2005).

[2] M. Eltschka, M. Wötzel, J. Rhensius, S. Krzyk, U. Nowak, M. Kläui, T. Kasama, R. E. Dunin-Borkowski, L. J. Heyderman, H. J. van Driel, and R. A. Duine, Phys. Rev. Lett. **105**, 056601 (2010).

[3] J.-S. Kim, O. Boulle, S. Verstoep, L. Heyne, J. Rhensius, M. Kläui, L. J. Heyderman, F. Kronast, R. Mattheis, C. Ulysse, and G. Faini, Phys. Rev. B **82**, 104427 (2010).

[4] C. Redondo, B. Sierra, S. Moralejo, and F. Castano, J. Magn. Magn. Mater. **322**, 1969 (2010).

[5] W. Zhang and S. Haas, Phys. Rev. B **81**, 064433 (2010).

[6] F. Q. Zhu, D. L. Fan, X. C. Zhu, J. G. Zhu, R. C. Cammarata, and C. L. Chien, Adv. Mater. **16**, 2155 (2004).

[7] A. Subramani, D. Geerpuram, A. Domanowski, V. Baskaran, and V. Metlushko, Physica C **404**, 241 (2004).

[8] J. Wang, A. O. Adeyeye, and N. Singh, Appl. Phys. Lett. **87**, 262508 (2005).

[9] A. Remhof, A. Schumann, A. Westphalen, H. Zabel, N. Mikuszeit, E. Y. Vedmedenko, T. Last, and U. Kunze, Phys. Rev. B **77**, 134409 (2008).

[10] A. Westphalen, A. Schumann, A. Remhof, H. Zabel, M. Karolak, B. Baxevanis, E. Y. Vedmedenko, T. Last, U. Kunze, and T. Eimüller, Phys. Rev. B **77**, 174407 (2008).

[11] X. S. Gao, A. O. Adeyeye, S. Goolaup, N. Singh, W. Jung, F. J. Castaño, and C. A. Ross, J. Appl. Phys. **101**, 09F505 (2007).

[12] P. Vavassori, M. Grimsditch, V. Novosad, V. Metlushko, and B. Ilic, Phys. Rev. B **67**, 134429 (2003).

[13] L. Thevenard, H. T. Zeng, D. Petit, and R. P. Cowburn, J. Magn. Magn. Mater. **322**, 2152 (2010).

[14] R. P. Cowburn, D. A. Allwood, G. Xiong, and M. D. Cooke, J. Appl. Phys. **91**, 6949 (2002).

[15] N. A. Usov, A. Zhukov, and J. Gonzalez, J. Magn. Magn. Mater. **316**, 255 (2007).

[16]P. Vavassori, R. Bovolenta, V. Metlushko, and B. Ilic, J. Appl. Phys. **99**, 053902 (2006).

[17]M. M. Soares, E. de Biasi, L. N. Coelho, M. C. dos Santos, F. S. de Menezes, M. Knobel, L. C. Sampaio, and F. Garcia, Phys. Rev. B **77**, 224405 (2008).

[18]T. G. Leong, A. M. Zarafshar, and D. H. Gracias, Small **6**, 792 (2010).

[19]E. Amaladass, B. Ludescher, G. Schütz, T. Tyliszczak, M.-S. Lee, and T. Eimüller, J. Appl. Phys. **107**, 053911 (2010).

[20]T. Blachowicz and A. Ehrmann, J. Appl. Phys. **110**, 073911 (2011).

[21]A. Tillmanns, S. Oertker, B. Beschoten, G. Güntherodt, C. Leighton, I. K. Schuller, and J. Nogués, Appl. Phys. Lett. **89**, 202512 (2006).

[22]T. Blachowicz, A. Ehrmann, P. Steblinski, and J. Palka, J. Appl. Phys. **113**, 013901 (2013).

[23]S.-J. Park, S. Kim, S. Lee, Z. G. Khim, K. Char, and T. Hyeon, J. Am. Chem. Soc. **122**, 8581–8582 (2000).

[24]W. Scholz, J. Fidler, T. Schrefl, D. Suess, R. Dittrich, H. Forster, and V. Tsiantos, Comput. Mater. Sci. **28**, 366–383 (2003).

[25]T. Blachowicz, A. Ehrmann neé Tillmanns, P. Steblinski, and L. Pawela, J. Appl. Phys. **108**, 123906 (2010).